2016

Optimal Heat Source Temperature For Supercritical Organic Rankine Cycle

Wei Liu
Institute for Energy Systems, Faculty of Mechanical Engineering, Technische Universität München, Germany, wei.liu@tum.de

Christoph Wieland
Institute for Energy Systems, Faculty of Mechanical Engineering, Technische Universität München, Germany, wieland@tum.de

Dominik Meinel
Institute for Energy Systems, Faculty of Mechanical Engineering, Technische Universität München, Germany,
dominik.meinel@tum.de

Hartmut Spliethoff
spliethoff@tum.de

Optimal Heat Source Temperature for Supercritical Organic Rankine Cycle

Wei LIU[1]*, Christoph WIELAND[1], Dominik MEINEL[1], Hartmut SPLIETHOFF[1,2]

[1]Institute for Energy Systems, Faculty of Mechanical Engineering, Technische Universität München
Boltzmannstrasse 15, 85748, Garching, Germany
E-mail: wei.liu@tum.de

[2]The Bavarian Center for Applied Energy Research (ZAE Bayern), Division 1: Technology for Energy Systems and Renewable Energy
Walther-Meissner-Str. 6, 85748, Garching, Germany
E-mail: spliethoff@tum.de

* Corresponding Author

ABSTRACT

Organic Rankine Cycle (ORC) enables power generation from low- to medium temperature heat sources. In an ORC, the organic medium shows different performances for different heat source temperatures. For a range of heat source temperatures, one temperature can be always identified corresponding to the best thermal match between the heat transfer fluid and working fluid. This temperature is defined as the Optimal Heat Source Temperature (OHST) and serves as an indicator for optimal efficiency. In this respect, the aim of this study is to investigate the OHST for supercritical fluid and its application in thermodynamic optimization. A simple ORC configuration is introduced and imposed with a set of constraints for establishing a cycle model. OHST is determined from parametric optimization and theoretical prediction, respectively. A comparative study is followed to examine the reliability of the theoretical prediction. In a subsequent case study, the OHST approach is compared with the conventional approach in thermodynamic optimization of a supercritical ORC. Optimal results from both approaches are compared, along with discussions and conclusions for further studies.

1. INTRODUCTION

Throughout the last decades, due to increasing concerns over un-ecological utilization of fossil fuels, exploitation of low-temperature heat source has attracted growing interest. A number of techniques are available that convert low-temperature heat to electricity. Among them, Organic Rankine Cycle (ORC) has been considered to be promising for several advantages, such as simplicity and high heat utilization efficiency (Quoilin *et al.,* 2013). In a typical ORC process (see figure 1a), the working medium loops in a closed cycle while the heat transfer fluid (HTF) cools down with a constant flow rate, transferring low-temperature heat to the cycle. The cycle performance depends on multi-parameters, such as the specification of heat source/sink, the choice of working fluid, and the operation conditions.

An important factor that influences the cycle performance is the heat transfer process between the heat source and the working fluid (Schuster *et al.,* 2010). Two parameters are often applied to describe the heat transfer process. The first one is the minimum temperature difference, also called the pinch point temperature, which has to be imposed to allow for an effective heat transfer. The second one is the exergy, indicating the maximum energy that can be obtained from the heat source medium until it reaches a dead state. In figure 1b the two parameters are qualitatively demonstrated. The pinch point occurs at the evaporator inlet for the working fluid, while the exergy is composed of three parts. The exergy destroyed due to irreversible heat transfer is defined as exergy destruction (Area I). The exergy wasted to the surrounding because of incomplete cooling of heat source is called exergy loss (Area II). The rest of the exergy flow is gained by the organic medium and hence is regarded as the useful exergy (Area III). Schuster *et al.* 2010 mentioned that the maximization of the power output of the ORC process is directly linked with the minimization of the discussed exergy destruction and loss. This could be realized by improving the thermal match between the heat source and the working fluid.

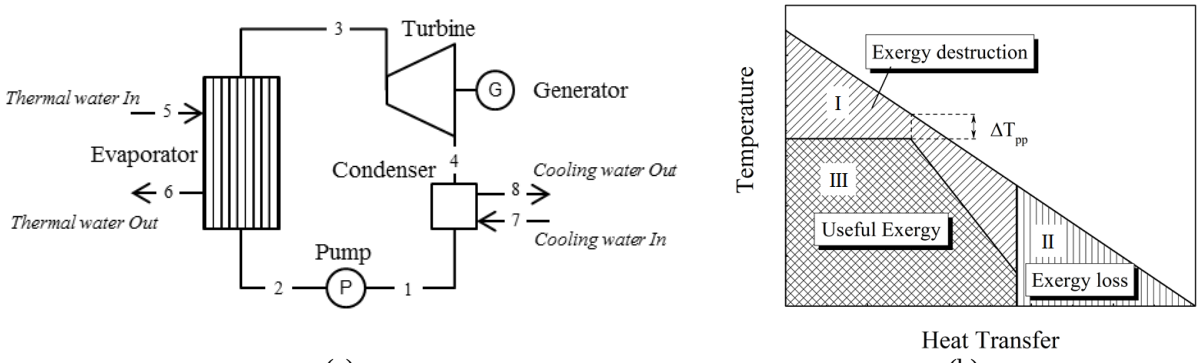

Figure 1: Schematic of a simple ORC and demonstration of exergy distribution in a heat transfer process.

A great limitation of improving the thermal match for a sub-critical ORC is the isothermal evaporation with enlarged temperature differences in area I (see figure 1b). By using a super-critical process such an isothermal evaporation can be avoided leading to a better thermal match, which can be perceived by comparing the TQ diagrams shown in figure 1b and figure 2a. Furthermore, the average temperature level of heat addition is increased, resulting in a larger enthalpy drop for a constant condensate pressure (Karellas *et al.*, 2008). In this respect, it is worthy of a further investigation on the super-critical ORC and its application in low temperature heat sources.

To date, quiet a number of studies are available, showing thermodynamic potential of supercritical ORC compared to the subcritical counterpart. Karellas *et al.* (2008) investigated supercritical ORC applications for different heat source temperatures. It was shown that the heat source temperature directly influences the choice of a suitable working fluid and its operation conditions. Schuster *et al.* (2010) carried out a theoretical study regarding the supercritical ORC for a heat source temperature of 210°C. It was found that the turbine inlet temperature has great impact on the discussed exergy distribution (see figure 1b) and hence on the system efficiency. Maraver *et al.* (2014) evaluated a set of fluids in a supercritical ORC process for different heat source temperatures, by taking into account multiple criteria. They concluded that working fluid whose critical temperature is much lower than the heat source temperature can be used with super-critical conditions, leading to high cycle efficiencies. However, oversized components are usually required, which increases manufacturing costs.

From the discussed literatures it can be inferred that a super-critical fluid could show different thermal performances for different heat source temperatures. In figure 2 three TQ diagrams are illustrated for an example fluid R227ea operating under same supercritical conditions but for different heat source temperatures. Due to the temperature dependence of heat capacity, the heat transfer process is discretized into a number of sections, each illustrated by the interval between i and i+1. In the case of low heat source temperature (figure 2a), the heat amount transferred to the cycle is constrained by the pinch point located close to the hot end of the heat transfer process. This results in a high outlet temperature of the heat source and hence a large amount of exergy loss. In the case of high heat source temperature (figure 2c), however, the pinch point is shifted to the cold end of the heat transfer process. As a result, exergy loss is almost minimized but exergy destruction is greatly increased (see figure 2c). To optimally balance the exergy destruction and loss, an Optimal Heat Source Temperature (OHST) can be always found, for which the total exergy destruction and loss is minimized and the thermal match reaches an optimum (figure 2b).

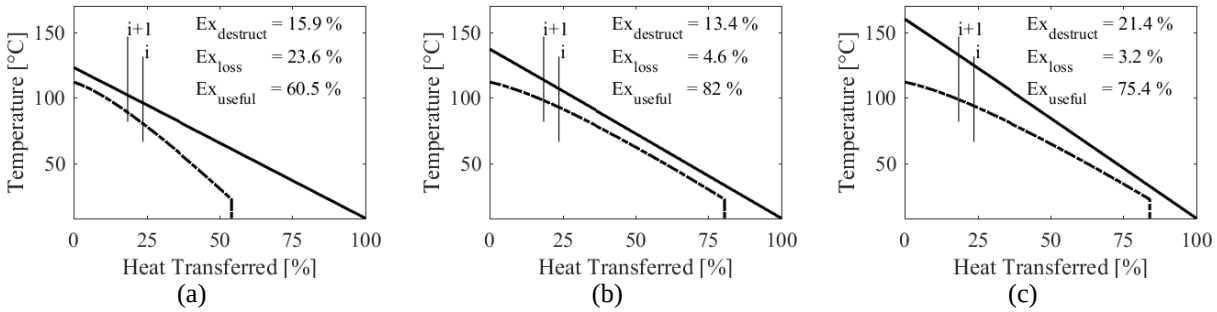

Figure 2: TQ diagram of an example fluid (R227ea), along with percentage distributions of exergy, and discretized heat transfer process.

The afore-described OHST and its application in thermodynamic optimization have been investigated by Liu *et al.*, (2015). However, their study focuses only on sub-critical ORC and no studies are so far available that investigate the OHST for a supercritical ORC. Therefore, the aim of this study is to extend the investigation of OHST from a sub-critical to a super-critical ORC, as well as to answer questions such as

a) For a supercritical ORC, is it true that the best fluids leading to the highest exergetic efficiencies are among those whose OHSTs are closer to the available heat source temperature?
b) How much do the optimization results (optimal fluid, optimal process parameter) obtained using the OHST approach deviate from the one using the conventional approach?
c) How much computational time can be saved by using OHST approach compared to the conventional one?

This study is structured as follows: section 2 gives a theoretical background of this study, in which two approaches of thermodynamic optimization are briefly reviewed, including a conventional one and an OHST one. In section 3 a cycle model, together with five evaluation parameters is introduced. In section 4 two methods are described for the determination of OHST, followed by results and conclusions for further numeric studies. Through a case study in section 5, the proposed OHST approach is demonstrated and compared with the conventional approach for optimization of a super-critical ORC process. Finally, conclusions are given in section 6, along with an outlook.

2. CYCLE OPTIMIZATION

2.1 Thermodynamic optimization: The conventional approach

The thermodynamic optimization using a conventional approach can be usually converted to a problem of Nonlinear Programming (NLP). In other words, for each of discrete variables (e.g. working fluid, cycle configuration), continuous variables (e.g. turbine inlet parameters) are optimized in a certain range of parameter space, leading to the maximal objective (e.g. net power output). Afterwards, fluids are ranked with the objectives, according to which optimal fluid and optimal parameters are identified. Obviously computational time using the conventional approach depends strongly on the number of the discrete variables, as well as the parameter space of the continuous variables.

2.2 Thermodynamic optimization: The OHST approach

When using the proposed OHST approach to solve such an optimization problem, the computational time can be greatly reduced by introducing a "pre-screening" process to the working fluid selection and additionally by narrowing the dimension of the initial parameter space. In the beginning of optimization, OHST is calculated for each candidate fluid by taking into account a wide range of operation parameters. The calculations are simultaneously done, since OHST can be correlated directly with state parameters (Liu *et al.*, 2015). A pre-screening process is followed, in which fluids with OHSTs closer to the available heat source temperature are selected. By adjusting OHST, optimal operation conditions are estimated, leading to a narrowed parameter space. The dimension of the narrowed parameter space depends strongly on the estimation accuracy. If the estimation could be accuracy enough, cycle optimization can be even neglected. At the end, a set of optimized objectives are resulted, according to which the optimal fluid and the optimal parameters are determined.

3. THERMODYNAMIC MODEL

3.1 Cycle Model

The cycle model considered in this study is based on a simple configuration, as shown in figure 1a. The working fluid at a saturated-liquid state (state 1) is pressurized to a supercritical pressure (state 2). Subsequently, it is led to an evaporator, absorbing heat from the hot fluid to be a super-heated vapor (state 3). The live vapor then expands in a turbine, rotating shaft and generating electricity. After the expansion, a super-heated vapor is generated (state 4) and led to a condenser where it is cooled down by a cold medium (e.g. water) to the saturated liquid (state 1).

Boundary conditions of the cycle model are summarized in table 1, under the assumptions that there is no heat loss and pressure drop in the components. For the heat input, thermal water is chosen as the heat transfer medium with a maximum pressure of 50 bar. Unlike the common cycle simulations, the thermal water temperature is regarded as a continuous variable and will be optimized for the determination of OHST. For the ORC process, working fluids are represented by nine fluids and they are ranked in a descending order of critical temperatures, as shown in table 2. The turbine inlet pressure is fixed at $1.02 \cdot p_c$ for each fluid (Schuster *et al.*, 2010). The condensation pressure is determined by the condensation temperature at 20 °C (Heberle *et al.*, 2015). For the heat sink, cooling water is used with an initial

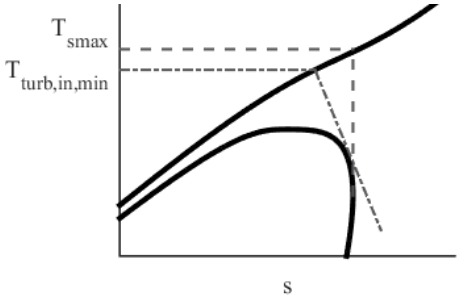

Figure 3: Minimum turbine inlet temperature in T-s-Diagram.

state of 1 bar and 8°C. The temperature level of the condensation system refers to the design point of the ORC plants in southern Bavaria, e.g. the geothermal ORC plant in Kirchstockach (Heberle *et al.*, 2015). Besides, the cycle simulation is performed in Matlab. Thermophysical properties are obtained from REFPROP 9.1 (Lemmon *et al.*, 2013).

In order for the fluid to expand without forming liquid droplets in the early stage of expansion, a minimum turbine inlet temperature ($T_{turb,in,min}$) has to be imposed, as demonstrated by the Temperature-entropy(T-s) diagram in figure 3. The determination of $T_{turb,in,min}$ depends not only on the saturation properties of the working fluid but also on the isentropic efficiency of turbine. For this reason, an iteration process is performed, in which T_{smax} (see figure 3) is input as the starting value and iteratively subtracted until the expansion line contacts the saturation line.

Under the given boundary conditions, the effect of $T_{turb,in}$ on OHST as well as cycle performance is investigated by a sensitivity analysis. It should be noted that the variation of $p_{turb,in}$ is not considered because evidences show that the turbine inlet temperature is more dominant to the cycle performance of supercritical ORC (Vetter *et al.*, 2013). However, such a parameter variation should be included in a future study.

3.2 Evaluation Criteria

Five evaluation criteria, i.e. system efficiency, exergetic efficiency in the evaporator, UA-value, pinch point position, size parameter of turbine are used in this study for performance evaluations.

System efficiency (η_{sys}) is regarded as an important criterion due to the combination of both thermodynamic efficiency and heat transfer efficiency of an ORC process (Schuster *et al.*, 2010). It is written as:

$$\eta_{sys} = \eta_{th} \cdot \eta_{HT} = \frac{P_{el,t} - P_{el,p}}{\dot{Q}_{hs}} = \frac{\eta_{mech} \cdot \eta_G \cdot (h_3 - h_4) - (h_2 - h_1)/\eta_{mech}/\eta_M}{h_5 - h_0} \quad (1)$$

where subscript 0 denotes the reference state, the other subscripts are related to the cycle presented in figure 1a.

Exergetic efficiency in the evaporator ($\eta_{ex,evp}$) is used to assess the thermal match between the heat transfer fluid and the working fluid (Liu *et al.*, 2015). It is given by:

$$\eta_{ex,HE} = \frac{\dot{m}_{wf}}{\dot{m}_{hs}} \cdot \frac{e_3 - e_2}{e_5 - e_0} \quad (2)$$

where the specific exergy flow e_i is calculated by $e_i = h_i - h - T_0 \cdot (s_i - s_0)$ (Schuster *et al.*, 2010):

UA-Value (UA), expressed as a product of heat transfer coefficient (U) and surface area (A), is considered due to its importance in cost evaluation of heat exchanger. As fluid varies substantially in terms of thermodynamic features especially at near pseudo-supercritical states, the heat transfer process with supercritical conditions is discretized into a number of sections with equal amount of heat flow ($\dot{Q}_i$), as demonstrated in figure 2. In the i^{th} section, heat capacity and transport properties are assumed equal to the mean value of the specific properties taken at point i and i+1. The number of section (N_{sec}) is set to be 100 to allow for acceptable predictive accuracy (Karellas *et al.*, 2008). Within the i^{th} section, the UA-value is described using the Log mean temperature difference (LMTD):

$$UA_i = \frac{\dot{Q}_i}{LMTD_i} = \frac{\dot{Q}_i \cdot \log(\Delta T_{i+1}/\Delta T_i)}{\Delta T_{i+1} - \Delta T_i} \quad (3)$$

It is worthy of note that knowing the UA-value cannot directly lead to prediction of the required surface area which is

Table 1: Boundary conditions for the cycle simulations.

Heat source temperature	T_{hs}	< 260 °C	Cooling water temperature	T_{cw}	8 °C
Heat source pressure	p_{hs}	< 5 MPa	Cooling water pressure	p_{cw}	1 bar
Heat source thermal amount	$\dot{Q}_{hs}$	1 MW	Isentropic efficiency Turbine	$\eta_{is,turbine}$	0.85
Turbine inlet pressure	$p_{turb,in}$	1.02·p_c bar	Isentropic efficiency Pump	$\eta_{is,pump}$	0.75
Pinch point in evaporator	$\Delta T_{pp,HE}$	10 K	Mechanical efficiency	η_{mech}	0.98
Condensation temperature	T_{cond}	20 °C	Generator/Motor efficiency	η_G/η_M	0.95
Pinch point in the condenser	ΔT_{cond}	5 K	Reference state	p_0, T_0	1 bar, 8 °C

Table 2: Fluid properties and the OHST-related characteristics. (Lemmon *et al.*, 2013)

Fluid	Tc °C	pc bar	MM g/mol	$c_{p,25°C}$ kJ/kgK	$T_{turb,in,min}$ °C	$OHST_{min}$ °C	$\overline{RD}$% $OHST_{cal}$
R1233zd	165.60	35.73	130.50	0.82	170.1	229.6	0.1
R245fa	154.0	36.5	134.0	0.9	157.6	213.0	-0.8
R1234zeZ	150.1	35.3	114.0	0.9	155.1	218.1	-1.4
R236ea	139.3	34.2	152.0	0.9	142.5	195.0	-1.2
R236fa	124.9	32.0	152.0	0.8	128.5	178.0	-2.4
R124	122.3	36.2	136.5	0.7	126.9	182.5	-4.3
R1234ze	109.4	36.3	114.0	0.9	114.6	170.7	-6.2
R227ea	101.8	29.3	170.0	0.8	104.6	149.3	-1.9
R1234yf	94.7	33.8	114.0	0.9	99.4	149.4	-4.7

more relevant with regard to cost evaluation. In this context, the UA-value serves only as an indicator to compare the required surface area, assuming a constant heat transfer coefficient U. To predict the surface area, a detailed calculation of U-value is necessary. Two studies are representative that provide models to estimate the U value of a supercritical heat transfer process (Karellas *et al.*, 2008, Lazova *et al.*, 2014).

Pinch point position (θ) is determined by identifying the minimum temperature difference ΔT_i related to equation 3. Here, it is characterized by a dimensionless parameter θ expressed as follows:

$$\theta = \dot{Q}_{pinch}/\dot{Q}_{orc} \tag{4}$$

where $\dot{Q}_{pinch}$ is the heat flow from the heat source inlet to the determined pinch point position, $\dot{Q}_{orc}$ is the heat amount transferred to the cycle. It is obvious that θ is a fraction between 0 and 1. A larger θ (and vice versa) indicates a pinch point position closer to the cold end of the evaporator related to figure 1a.

Size parameter (SP) is linked directly with the actual turbine dimensions and hence of great interest for the turbine design (Angelino *et al.*, 1984). The SP is defined as:

$$SP = \sqrt{\dot{V}_{out,exp}}/\Delta h_{is}^{1/4} \tag{5}$$

4. OPTIMAL HEAT SOURCE TEMPERATURE

4.1 OHST from parametric optimizations

Once a turbine inlet temperature ($T_{turb,in}$) is given, exergetic efficiency in the evaporator $\eta_{ex,evp}$ varies only with heat source temperatures (T_{hs}) in the current model (see figure 2). Therefore, the Optimal Heat Source Temperature (OHST) is obtained from a one-dimensional optimization, described in a mathematical form of:

$$\max(\eta_{ex,evp}) = f(T_{hs}) \tag{6}$$

The optimization focuses on the heat transfer process in evaporator. The method is to iterate the T_{hs}, along with a number of process simulations, until $\eta_{ex,evp}$ is maximized. The number of iterations depends on the initial parameter space of T_{hs}, the algorithm used in the optimization, as well as the termination tolerance. The optimization was performed in Matlab using the function handle "fminbnd". To define the parameter space of T_{hs}, the upper boundary was chosen to be 260°C in order to avoid phase change for thermal water. The lower boundary, depending on the specific working fluid, was equal to the minimum heat source temperature that allows for super critical operation. The "Golden Section Search" was selected as the optimization algorithm (Forsythe *et al.*, 1977). The termination tolerance of $\delta=10^{-2}$ was specified for T_{hs}, corresponding to the lower bound on the size of an optimization step.

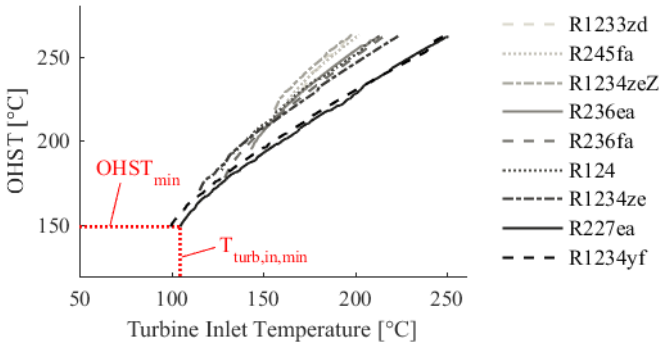

Figure 4: OHST as a function of $T_{turb,in}$ for the investigated fluids. The $OHST_{min}$ is demonstrated for R227ea.

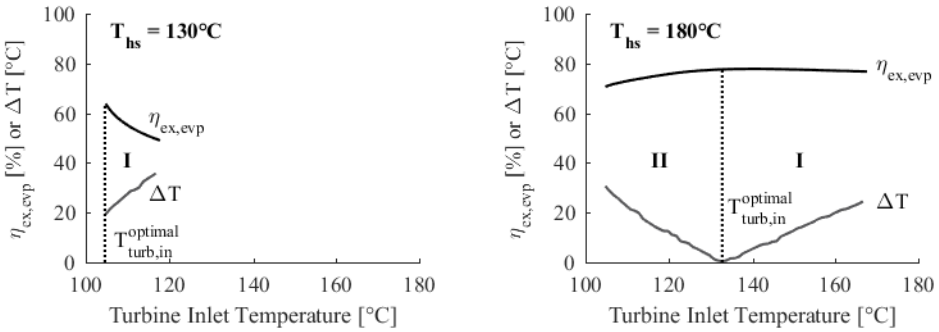

(a) (b)

Figure 5: $\eta_{ex,evp}$ and ΔT as a function of $T_{turb,in}$ in case of (a) T_{hs} = 130 °C and (b) T_{hs} = 180 °C. (Note: Region I indicates rising ΔT, while region II decreasing ΔT.)

A sensitivity analysis was followed, in which $T_{turb,in}$ was increased from $T_{turb,in,min}$ with a ramp of 1 °C, until the corresponding OHST reached the upper boundary of T_{hs} (260 °C). Figure 4 shows the resulting OHSTs as a function of $T_{turb,in}$. In general, fluids with higher critical temperatures are observed with higher OHSTs. For each fluid, OHST increases monotonically with rising turbine inlet temperatures. Therefore, a minimum OHST ($OHST_{min}$) can be always found at $T_{turb,in,min}$, as shown in figure 4 for R227ea. A summarization of $OHST_{min}$ can be found in table 2.

To demonstrate the significance of OHST in cycle optimization, a sensitivity analysis was carried out for R227ea, in which the influence of $T_{turb,in}$ on the $\eta_{ex,evp}$ was investigated. Two heat source temperatures (T_{hs}= 130°C and 180°C) were considered for the current cycle model. For each T_{hs}, $T_{turb,in}$ was increased from $T_{turb,in,min}$ to its upper limit which depends on the pinch point temperature. To link the OHST with the investigated cycles, the absolute value of temperature difference between T_{hs} and OHST was calculated:

$$\Delta T = \left| T_{hs} - OHST\left(T_{turb,in}\right) \right| \tag{7}$$

where T_{hs} is a constant (130 °C or 180°C), and OHST is a function of $T_{turb,in}$ as shown in figure 4.

In figure 5, $\eta_{ex,evp}$ and ΔT as a function of $T_{turb,in}$ are displayed for the investigated T_{hs}, respectively. It is observed that the influence of $T_{turb,in}$ on $\eta_{ex,evp}$ is strongly related with the variation of ΔT. The maximal $\eta_{ex,evp}$ occurs at a certain $T_{turb,in}$ where ΔT is minimized. In the case of a rising ΔT, $\eta_{ex,evp}$ decreases with increasing $T_{turb,in}$, which can be seen in figure 5a and figure 5b for region I. In the case of a decreasing ΔT, however, $\eta_{ex,evp}$ increases monotonically with an increasing $T_{turb,in}$, as shown in figure 5b for region II. As a result, $\eta_{ex,evp}$ reaches the maximum at a certain $T_{turb,in}$ that corresponds to the minimum of ΔT. This $T_{turb,in}$ is in turn defined as the optimal $T_{turb,in}$, as demonstrated in figure 5.

Summarizing, OHST is a function of turbine inlet temperature for fluids with super-critical conditions. In an optimization model in which T_{hs} is given, the minimization of the absolute value of the difference between OHST and T_{hs} (ΔT in equation 7) indicates the maximization of $\eta_{ex,evp}$ and the optimal $T_{turb,in}$. This conclusion is regarded as the significance of OHST and will be applied to the following case study.

4.2 OHST from Theoretical Calculation

The determination of OHST from parametric optimizations is based on a large number of cycle simulations with different heat source temperatures. It is therefore a time-consuming process and no algorithms are reliable that can notably reduce the running time. On this account, we tried to find a method, using which OHST can be theoretically estimated without cycle simulation.

For a sub-critical ORC, a mathematical form (Liu *et al.*, 2015)

$$OHST_{sub} = \frac{h_{evp}}{\bar{c}_{p,pre,wf}} + T_{evp} + \Delta T_{pp} \tag{8}$$

was derived to predict the OHST, with the following assumptions: 1) dependence of the heat capacity on temperature is neglected; 2) parallel temperature profile in the preheating process. This equation implies that for a sub-critical fluid, OHST is a parameter depending only on fluid parameters and the pinch point temperature in evaporator. Compared to the OHSTs obtained from optimizations, the OHSTs obtained using equation 8 show only an average Relative Deviation (RD) of 0.81%. The RD% is defined as:

$$RD\% = \frac{OHST_{cal} - OHST_{opt}}{OHST_{opt}} \times 100\% \tag{9}$$

where the subscript "cal" refers to the OHST calculated e.g. using equation 8, while "opt" indicates the OHST obtained from parametric optimization.

Likewise, for a super-critical ORC, a theoretical formula may be written with the same assumptions made to the sub-critical fluid:

$$OHST_{super} = \frac{h_{turb,in} - h_{tc}}{\bar{c}_{p,pre,wf}} + T_c + \Delta T_{pp} \tag{10}$$

where h_{tc} is the specific enthalpy obtained with the critical temperature, $\bar{c}_{p,pre,wf}$ is the average heat capacity of the fluid at liquid states (i.e. preheating process).

To allow equation 10 for further applications, a comparative study was performed, in which OHSTs were calculated for increasing $T_{turb,in}$ using equation 10 and compared with those obtained from the parametric optimizations (see figure 4). In table 2, the mean values of the RD% (denoted as $\overline{RD}\%$) of the calculated $OHST_{super}$ are shown, representing the predictive accuracy of equation 10. In general, high deviations (up to 6.2%) are observed due to the fact that for a super-critical fluid the heat capacity varies strongly with temperature and hence the assumptions made in equation 8 cannot be applied. However, equation 10 can be still acceptable for engineering purposes. In a next step, the observed deviations and their influences on the final optimization results will be discussed to better appreciate the accuracy of equation 10.

5. CASE STUDY

The conventional approach and the OHST approach are respectively applied to the thermodynamic optimization of a super-critical ORC process. Cycle model is the same as described in section 3 except for the thermal water which is defined with an initial condition of 180°C and 10 bar. The common aim of both approaches is to maximize one optimization objective ($\eta_{ex,evp}$) by iterating one discrete variable (working fluid) and one continuous variable (turbine inlet temperature). The optimal decisions resulting from both approaches, i.e. optimal working fluids and optimal operation conditions are compared and analyzed.

5.1 Thermodynamic optimization: the conventional approach

Thermodynamic optimizations using the conventional approach were performed on the basis of the function handle "fminbnd". The parameter space of $T_{turb,in}$ was determined differently for the considered fluids. While the lower bound of $T_{turb,in}$ was set to $T_{turb,in,min}$ (see table 2), the upper bound of $T_{turb,in}$ was set to $T_{hs} - \Delta T_{pp}$. The optimization algorithm and termination tolerance on $T_{turb,in}$ were kept the same as the one-dimensional optimization, as stated in section 4.

Table 3 shows the optimized $T_{turb,in}$ for the investigated fluids, along with corresponding cycle characteristics. The computational time using the conventional approach (2723.1 seconds) was recorded and would be compared with the OHST approach. It should be noted that no results are observed for R1233zd because the minimum turbine inlet temperature (170.1°C) is so high that a pinch point temperature of 10 °C cannot be realized in the evaporator. With the highest exergetic efficiency of 83.87%, R236fa can be identified as the optimal fluid with an optimal $T_{turb,in}$ of

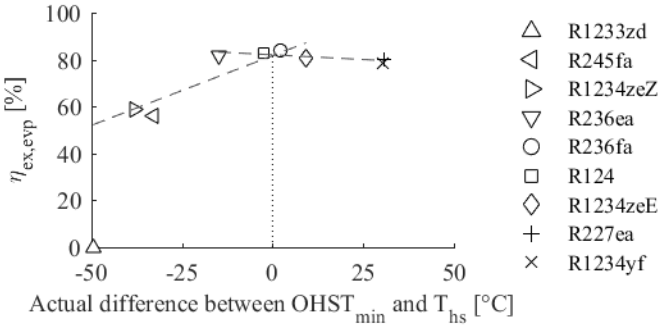

Figure 6: Optimized $\eta_{ex,evp}$ versus the actual difference between T_{hs} and $OHST_{min}$ (T_{hs} - $OHST_{min}$).

Table 3: Results from the optimizations using the conventional and OHST approach.

Fluid	$p_{turb,in}$	$T_{turb,in}$ [°C]		η_{sys} [%]		$\eta_{ex,HE}$ [%]		θ [-]		$\overline{UA}$ [W/K]		SP [cm]	
	bar	C*	O*	C	O	C	O	C	O	C	O	C	O
R1233zd	-	-	-	-	-	-	-	-	-	-	-	-	-
R245fa	37.24	157.65	-	8.24	-	56.22	-	0.22	-	230.1	-	3.5	-
R1234zeZ	36.04	155.12	-	8.66	-	58.75	-	0.27	-	248.1	-	3.3	-
R236ea	34.88	142.51	142.92	11.69	11.59	81.95	81.27	0.41	0.39	537.3	520.1	4.1	4.0
R236fa	**32.64**	**129.41**	**130.08**	**11.77**	**11.76**	**83.87**	**83.82**	**0.72**	**0.68**	**618.0**	**615.5**	**4.0**	**3.9**
R124	36.97	126.95	128.36	11.66	11.64	82.96	82.65	0.67	0.62	592.2	578.9	3.5	3.5
R1234zeE	37.08	123.20	129.22	11.10	11.01	80.34	80.08	0.72	0.64	545.5	521.9	3.0	2.9
R227ea	29.84	139.81	-	9.61	-	80.11	-	0.67	-	510.3	-	3.1	-
R1234yf	34.50	165.49	-	9.04	-	78.54	-	0.65	-	425.0	-	2.4	-

*C: conventional approach; *O: OHST approach

129.41°C. Under optimal conditions, the highest system efficiency is observed as well, which supports the conclusion that system efficiency is directly linked with the exergetic efficiency in the evaporator. Besides, a large θ value (equation 4) indicates a pinch point position closer to the cold end of evaporator. This is a result of the tradeoff between the exergy destruction and the exergy loss, related to figure 1a. The main drawbacks of using the optimal fluid are twofold, both concerning economic aspects. First, a high UA-value is observed, indicating a high surface area required for the evaporator with the assumption of a constant U-value. Taking into account the fact that heat transfer coefficient deteriorates with increasing superheating temperatures (Karellas *et al.*, 2008), an even larger surface area is possible in reality. Furthermore, a high Size Parameter of Turbine (SP) is seen, which implies the necessity of larger turbine blades. Both large surface area and large turbine blades could cause high manufacture costs.

In addition, it can be seen that the fluids whose $OHST_{min}$ (see table 2) are closer to the investigated heat source temperature (180°C) can lead to the highest $\eta_{ex,evp}$. To better present this observation, the optimized $\eta_{ex,evp}$ are plotted versus the actual differences between the $OHST_{min}$ and the T_{hs}, as shown in figure 6. Four fluids, namely R236ea, R236fa, R124, R1234zeE are found with the highest efficiencies and their $OHST_{min}$ are indeed closest to the T_{hs}. This observation justifies the assumption of question a) we raised in section 1, and in a next step, it will be applied to the following OHST approach.

5.2 Thermodynamic optimization: the OHST approach

The OHST approach is used independently from the conventional approach. It is based only on the theoretical formula in equation 10 and the conclusions/assumptions that have been made in the previous sections:

rule 1. Fluids with $OHST_{min}$ (table 2) closer to the available heat source temperature are the optimal ones leading to the highest exergetic efficiencies in evaporator;

rule 2. The maximization of exergetic efficiency in evaporator is linked with the minimization of the absolute value of the difference between OHST and T_{hs} (i.e. ΔT in equation 7).

The optimization process is described in five steps, as stated in the following: Step 1: predict $OHST_{min}$ (equation 10); Step 2: pre-screening process (rule 1); Step 3: identify optimal $T_{turb,in}$ for the fluids obtained in step 2 (rule 2); Step 4: insert optimal $T_{turb,in}$ to the cycle model; Step 5: rank fluids & make optimal decision.

In step 1, $OHST_{min}$ were obtained using equation 10. In step 2, a pre-screening process was imposed by comparing the calculated $OHST_{min}$ with the given heat source temperature. As a result, four fluids (i.e. R236ea, R236fa, R124, R1234zeE) were selected for further optimizations as their $OHST_{min}$ were closest to the heat source temperature. In step 3, $T_{turb,in}$ was adjusted in such a way, that the absolute value of the difference between the corresponding OHST and T_{hs} is minimized. More specifically, in the case where $OHST_{min} > T_{hs}$, the minimum of $T_{turb,in}$ was chosen. In the case where $OHST_{min} < T_{hs}$, turbine inlet temperature was increased from its minimum to a certain point at which the corresponding OHST equals T_{hs}. In step 4, the $T_{turb,in}$ obtained in step 3 were inserted to the cycle model, leading to a set of performance parameters, as shown in table 3. Finally, in step 5, the investigated fluids were ranked in a decreasing order of their $\eta_{ex,evp}$ and hence the optimal decision can be made with the optimal fluid and the optimal T_{hs}.

Using the OHST approach, R236fa was also identified as the optimal fluid. The optimal $T_{turb,in}$ is 130.08°C, which shows a RD of 0.52% compared to the $T_{turb,in}$ in the conventional optimization. Furthermore, the RD of $T_{turb,in}$ would lead to deviations with regard to the performance parameters. In the discussed model, 0.11% is observed for the RD of η_{sys}, 0.05% for the RD of $\eta_{exe,HE}$, -5.5% for the RD of θ, 0.40% for the RD of $\overline{UA}$ and -0.70% for the RD of SP. These observations suggest that the optimization results obtained with the OHST approach are in a good agreement with the conventional approach, which in turn provides the answer to the question b) that we raised in section 1. Moreover, the computational time (77.4 seconds) using the OHST approach is significantly reduced in contrast to that using the conventional approach (2723.1 seconds). Obviously computational time can be saved due to the fact that the OHST approach requires almost no cycle simulations for determining the optimal results. Cycle simulations are required only for the performance evaluations.

6. CONCLUSIONS

A systematic study was carried out, showing the potential of using the Optimal Heat Source Temperature (OHST) approach in the thermodynamic optimization of super-critical ORC processes. Based on the heat transfer process in the evaporator, an optimization model has been developed and used for the determination of OHST. Results show that the OHST for a super-critical ORC increases monotonically with increasing turbine inlet temperatures. The significance of OHST in thermodynamic optimization was demonstrated by simulating an exemplary fluid for two different heat source temperatures. It was found that the maximization of exergetic efficiency in the evaporator ($\eta_{ex,evp}$) is linked directly with the minimization of the absolute value of the difference between OHST and T_{hs} (ΔT in equation 7). This finding/rule was later applied to a case study, determining optimal turbine inlet temperatures. In order to shorten the computational time of OHST, a theoretical formula was derived (see equation 10), correlating OHST with fluid properties under super-critical conditions. A subsequent comparative study shows that the predictive reliability of the theoretical formula is acceptable for engineering purposes. The OHST approach, together with the conventional approach was successfully applied to a case study. It was found that optimal fluids are among those whose minimal OHSTs ($OHST_{min}$) are closer to the available heat source temperature. By using the OHST approach, the computational time was significantly reduced, along with the same optimal fluid (R236fa) and similar optimal parameters.

Although the OHST approach has been proven effective for optimizing super-critical ORCs, challenges remain ahead. To improve the current model, a minimum heat source outlet temperature (e.g. dew point) should be specified for some real ORC applications. Furthermore, the recuperator is one of the most relevant components in a real ORC process, and it should be also added as a discrete parameter to the current model. In addition, the effect of turbine inlet pressure on OHST should be also investigated for the current model.

NOMENCLATURE

c_p	Specific heat capacity	(kJ/kg·K)	SP	Size Paramter	(cm)
e	Specific exergy flow	(kJ/kg)	UA	Heat transfer conductance	(W/K)
h	Specific enthalpy	(kJ/kg)			
m	Mass flow rate	(kg/s)	*Greek letters*		
p	Pressure or power	(bar or kW)	θ	Pinch point position	(-)
$\dot{Q}$	Heat flow	(MW)	η	Efficiency	(%)
s	Specific entropy	(kJ/kgK)	*Acronyms*		
T	Temperature	(°C)	LMTD	Logarithmic Mean Temperature Difference	
V	Volume flow rate	(m3/s)	OHST	Optimal Heat Source Temperature	

Subscript

0,1,2,…10	Reference or working states	is	isentropic
c	critical	M	motor
cw	cold water	min	minimum
cond	condensation	mech	mechanical
el	electricity	out	out
evp	Evaporation	pp	pinch point
exe	Exergy	pre	preheater
exp	expander	sec	section
G	Generator	sys	system
hs	Heat source	th	thermal
HE	Heat Exchanger	turb	turbine
in	inlet	wf	working fluid

REFERENCES

Angelino, G., Gaia, M., & Macchi, E. (1984). A review of Italian activity in the field of organic Rankine cycles. *VDI-Berichte*, (539), 465-482.

Forsythe, G. E., Malcolm, M. A., & Moler, C. B. Computer Methods for Mathematical Computations. *Journal of applied mathematics and mechanics: Zeitschrift für angewandte Mathematik und Mechanik 59*(2):141-142

Heberle, F., & Brüggemann, D. (2010). Exergy based fluid selection for a geothermal Organic Rankine Cycle for combined heat and power generation. *Applied Thermal Engineering, 30*(11), 1326-1332.

Heberle, F., Preißinger, M., & Brüggemann, D. (2012). Zeotropic mixtures as working fluids in Organic Rankine Cycles for low-enthalpy geothermal resources. *Renewable Energy, 37*(1), 364-370.

Heberle, F., Jahrfeld, T., & Brüggemann, D. (2015) Thermodynamic Analysis of Double-Stage Organic Rankine Cycles for Low-Enthalpy Sources Based on a Case Study for 5.5 MWe Power Plant Kirchstockach. *Proceedings World Geothermal Congress, Melbourne* (Australia).

Karellas, S., & Schuster, A. (2008). Supercritical fluid parameters in organic Rankine cycle applications. *International Journal of Thermodynamics, 11*(3), 101-108.

Lazova, M., Daelman, S., Kaya, A., Huisseune, H., & De Paepe, M. (2014). Heat transfer in horizontal tubes at supercritical pressures for organic Rankine Cycle applications. *International Conference on Heat Transfer, Fluid Mechanics and Thermodynamics* (1044-1050). Florida.

Lemmon, E. W., Huber, M. L., & McLinden, M. O. (2013) NIST Standard Reference Database 23: Reference Fluid Thermodynamic and Transport Properties-REFPROP, Version 9.1, Standard Reference Data Program; *National Institute of Standards and Technology: Gaithersburg*, MD.

Liu, W., Meinel, D., Wieland, C., & Spliethoff, H. (2014). Investigation of hydrofluoroolefins as potential working fluids in organic Rankine cycle for geothermal power generation. *Energy, 67*, 106-116.

Liu, W., Meinel, D., Gleinser, M., Wieland, C., & Spliethoff, H. (2015). Optimal Heat Source Temperature for thermodynamic optimization of sub-critical Organic Rankine Cycles. *Energy, 88*, 897-906.

Maraver, D., Royo, J., Lemort, V., & Quoilin, S. (2014). Systematic optimization of subcritical and transcritical ORCs constrained by technical parameters in multiple applications. *Applied energy, 117*, 11-29.

Quoilin, S., Van Den Broek, M., Declaye, S., Dewallef, P., & Lemort, V. (2013). Techno-economic survey of Organic Rankine Cycle (ORC) systems. *Renewable and Sustainable Energy Reviews, 22*, 168-186.

Schuster, A., Karellas, S., & Aumann, R. (2010). Efficiency optimization potential in supercritical Organic Rankine Cycles. *Energy, 35*(2), 1033-1039.

Vetter, C., Wiemer, H. J., & Kuhn, D. (2013). Comparison of sub-and supercritical Organic Rankine Cycles for power generation from low-temperature/low-enthalpy geothermal wells considering specific net power output and efficiency. *Applied Thermal Engineering, 51*(1), 871-879.

ACKNOWLEDGEMENT

This work was supported by Danish Council for Strategic Research under the THERMCYC project ("Advanced thermodynamic cycles utilising low-temperature heat sources"; No. 1305-00036B). The financial support is gratefully acknowledged.